



HAL
open science

Hepatic deletion of serine palmitoyl transferase 2 impairs ceramide/sphingomyelin balance, bile acids homeostasis and leads to liver damage in mice

Justine Lallement, Ilyès Raho, Grégory Merlen, Dominique Rainteau, Mikael Croyal, Melody Schiffano, Nadim Kassis, Isabelle Doignon, Maud Soty, Floriane Lachkar, et al.

► To cite this version:

Justine Lallement, Ilyès Raho, Grégory Merlen, Dominique Rainteau, Mikael Croyal, et al.. Hepatic deletion of serine palmitoyl transferase 2 impairs ceramide/sphingomyelin balance, bile acids homeostasis and leads to liver damage in mice. *Biochimica et Biophysica Acta Molecular and Cell Biology of Lipids*, 2023, 1868 (8), pp.1-13. 10.1016/j.bbalip.2023.159333 . hal-04282229

HAL Id: hal-04282229

<https://cnrs.hal.science/hal-04282229>

Submitted on 14 Nov 2023

HAL is a multi-disciplinary open access archive for the deposit and dissemination of scientific research documents, whether they are published or not. The documents may come from teaching and research institutions in France or abroad, or from public or private research centers.

L'archive ouverte pluridisciplinaire **HAL**, est destinée au dépôt et à la diffusion de documents scientifiques de niveau recherche, publiés ou non, émanant des établissements d'enseignement et de recherche français ou étrangers, des laboratoires publics ou privés.

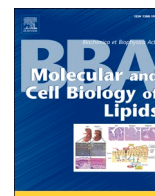


Distributed under a Creative Commons Attribution - NoDerivatives 4.0 International License



Contents lists available at ScienceDirect

BBA - Molecular and Cell Biology of Lipids

journal homepage: www.elsevier.com/locate/bbalip

Hepatic deletion of serine palmitoyl transferase 2 impairs ceramide/sphingomyelin balance, bile acids homeostasis and leads to liver damage in mice

Justine Lallement^a, Ilyès Raho^a, Grégory Merlen^b, Dominique Rainteau^c, Mikael Croyal^{d,e,f}, Melody Schiffano^f, Nadim Kassis^a, Isabelle Doignon^b, Maud Soty^g, Floriane Lachkar^h, Michel Krempfⁱ, Matthias Van Hul^{j,k}, Patrice D. Cani^{j,k}, Fabienne Foufelle^h, Chloé Amouyal^a, Hervé Le Stunff^l, Christophe Magnan^{a,1}, Thierry Tordjmann^{b,1}, Céline Cruciani-Guglielmacci^{a,*,1}

^a Université Paris Cité, CNRS, Unité de Biologie Fonctionnelle et Adaptative, F-75013 Paris, France

^b Université Paris-Saclay, Inserm U1193, Orsay, France

^c Sorbonne Université, Inserm, Centre de Recherche Saint-Antoine, CRSA, AP-HP, Hôpital Saint Antoine, Biochemistry Department, Paris, France

^d Université de Nantes, CHU Nantes, CNRS, INSERM, l'institut du thorax, F-44000 Nantes, France

^e Université de Nantes, CHU Nantes, Inserm, CNRS, SFR Santé, Inserm UMS 016, CNRS UMS 3556, F-44000 Nantes, France

^f Plateforme de Spectrométrie de Masse du CRNH-O, UMR1280, Nantes, France

^g Université Claude Bernard Lyon 1, Université de Lyon, INSERM UMR-S1213, Lyon, France

^h Centre de Recherche des Cordeliers, INSERM, Sorbonne Université, 75006 Paris, France

ⁱ Clinique Bretéché, Groupe Elsan, Nantes, France

^j Metabolism and Nutrition Research Group, Louvain Drug Research Institute, UCLouvain (Université catholique de Louvain), 1200 Brussels, Belgium

^k Walloon Excellence in Life Sciences and BIOTEchnology (WELBIO) department, WEL Research Institute (WELRI), avenue Pasteur, 6, 1300 Wavre, Belgium

^l Institut des Neurosciences Paris-Saclay, CNRS UMR 9197, Université Paris Saclay, France

ARTICLE INFO

Keywords:

Ceramides

Liver

Sphingomyelinase

Bile acids

Gluconeogenesis

Fibrosis

ABSTRACT

Ceramides (Cer) have been shown as lipotoxic inducers, which disturb numerous cell-signaling pathways, leading to metabolic disorders such as type 2 diabetes. In this study, we aimed to determine the role of *de novo* hepatic ceramide synthesis in energy and liver homeostasis in mice. We generated mice lacking serine palmitoyltransferase 2 (*Spltc2*), the rate limiting enzyme of ceramide *de novo* synthesis, in liver under albumin promoter. Liver function, glucose homeostasis, bile acid (BA) metabolism and hepatic sphingolipids content were assessed using metabolic tests and LC-MS. Despite lower expression of hepatic *Spltc2*, we observed an increased concentration of hepatic Cer, associated with a 10-fold increase in neutral sphingomyelinase 2 (nSMase2) expression, and a decreased sphingomyelin content in the liver. *Spltc2*^{ALiv} mice were protected against obesity induced by high fat diet and displayed a defect in lipid absorption. In addition, an important increase in tauro-muricholic acid was associated with a downregulation of the nuclear BA receptor FXR target genes. *Spltc2* deficiency also enhanced glucose tolerance and attenuated hepatic glucose production, while the latter effect was

Abbreviations: Akt/Pkb, Protein Kinase B; Alat, alanine amino-transferase; Asat, aspartate amino-transferase; BA, bile acids; Bax, Bcl-2-associated X protein; Bcl2, B-cell lymphoma 2; cAMP, cyclic adenosine monophosphate; CDCA, chenodeoxycholic acid; Cer, ceramides; CerS, ceramide synthase; Chop, C/EBP homologous protein; Ck19, cytokeratin 19; CycloA, cyclophilin A; ECM, extracellular matrix; EDL, extensor digitorum longus; ER, endoplasmic reticulum; FFA, free-fatty acid; Fxr, farnesoid X receptor; G6p, glucose-6-phosphate; G6pase, glucose-6-phosphatase; GlyTT, glycerol tolerance test; Gpr78, G-protein coupled receptor 78; Gr-1, granulocyte receptor-1; HFD, high fat diet; ITT, insulin tolerance test; KD, knock-down; NASH, non-alcoholic steatohepatitis; nSMase2, neutral sphingomyelinase 2; OGTT, oral glucose tolerance test; Pc, pyruvate carboxylase; PTT, pyruvate tolerance test; RC, regular chow; S1pr2, sphingosine-1-phosphate receptor 2; SEM, standard error of the mean; SL, sphingolipid; SM, sphingomyelin; Smase, sphingomyelinase; Smpd3, sphingomyelin phosphodiesterase 3; Spt, serine palmitoyl-transferase; T2D, type 2 diabetes; Tbp, TATA-binding protein; Tgr5, Takeda G protein-coupled receptor; T-MCA, tauro-muricholic acid; Tnfr-1, TNF receptor 1; Tnfr, tumor necrosis alpha; T-β-MCA, tauro-beta-muricholic acid; WT, wild type.

* Corresponding author at: Université Paris Cité, 4 rue Marie-Andrée Lagroua Weill-Halle, 75205 Paris cedex 13, France.

E-mail address: celine.cruciani@u-paris.fr (C. Cruciani-Guglielmacci).

¹ These authors contributed equally to this work.

<https://doi.org/10.1016/j.bbalip.2023.159333>

Received 29 September 2022; Received in revised form 24 February 2023; Accepted 30 April 2023

Available online 22 May 2023

1388-1981/© 2023 The Authors. Published by Elsevier B.V. This is an open access article under the CC BY-NC-ND license (<http://creativecommons.org/licenses/by-nc-nd/4.0/>).

dampened in presence of nSMase2 inhibitor. Finally, *Sptlc2* disruption promoted apoptosis, inflammation and progressive development of hepatic fibrosis, worsening with age. Our data suggest a compensatory mechanism to regulate hepatic ceramides content from sphingomyelin hydrolysis, with deleterious impact on liver homeostasis. In addition, our results show the involvement of hepatic sphingolipid modulation in BA metabolism and hepatic glucose production in an insulin-independent manner, which highlight the still under-researched role of ceramides in many metabolic functions.

1. Introduction

In the last few decades, number of studies have pointed out deleterious roles of ceramides (Cer) especially in the development of metabolic disorders such as non-alcoholic steatohepatitis (NASH) or type 2 diabetes (T2D) [1]. Thus, this specific class of lipids, which belongs to sphingolipids (SL) family, are proposed to be important mediators of free-fatty acid (FFA)-induced β cell dysfunction and apoptosis, and FFA-induced insulin resistance in insulin target tissue [2]. At the cellular level, increased concentrations of Cer promote insulin resistance by inhibiting insulin signaling pathway, and Cer can regulate autophagy, reactive oxygen species production, cell proliferation, inflammation and apoptosis [3].

In mammals, three main pathways have been described to produce Cer. First, the *de novo* synthesis pathway starts on the cytoplasmic face of the endoplasmic reticulum (ER) with the condensation of a coenzyme A-linked fatty acid (palmitoyl-CoA) and L-serine by serine palmitoyl-transferase (SPT) to form 3-ketosphinganine. Three different subunits of SPT called SPTLC1, SPTLC2, and SPTLC3 have been described. SPTLC1 could act as a dimer with SPTLC2 and/or SPTLC3, which carry out the pyridoxal 5-phosphate binding motif, essential for the catalytic activity [4]. Then, Cer are transported to the Golgi apparatus to be metabolized into more complex sphingolipids such as glucosylceramides and sphingomyelin (SM). Second, the catabolic sphingomyelinase (SMase) pathway leads to the degradation of SM into Cer and takes place at different sub-cellular localizations (plasma membrane, mitochondria, lysosome and Golgi) [5]. The third pathway is called the “salvage pathway” from late endosomes/lysosomes, which generate Cer from the breakdown of complex sphingolipids [6]. In both salvage and *de novo* synthesis pathways, Cer are produced by ceramide synthase (CerS) through N-acylation of a sphingoid base. There are six different isoforms of CerS, which lead to the production of different Cer species, according to the chain length of the acyl-CoA added [7]. Among them, C18:0-Cer and C16:0-Cer have been pointed out as apoptosis and inflammatory inducers and play a key role in the development of insulin resistance [8–10].

The liver is a key metabolic organ, which governs body energy metabolism. In particular, the intrahepatic accumulation of lipids, especially Cer, strongly correlates with the risk of T2D [11]. In addition, it has been demonstrated that *in vivo* or *in vitro* inhibition of SPT, using myriocin, decreases Cer accumulation in plasma and liver and improves hepatic fibrosis, steatosis and insulin sensitivity [12,13]. Hepatocytes, the major parenchymal cells in the liver, carry out many metabolic functions, including the production of bile acids (BA). BA are amphipathic molecules, which allow dietary lipid absorption and also act as signaling molecules through their action on nuclear receptors such as the Farnesoid X receptor (FXR) or G protein-coupled BA receptors, such as Takeda G protein-coupled receptor 5 (TGR5) or S1P receptor 2 (S1PR2) [14,15]. FXR is activated by chenodeoxycholic acid (CDCA) but inhibited by tauro-beta-muricholic acid (T- β -MCA), and regulates BA synthesis [16,17]. Numerous studies have demonstrated the role of FXR signaling in glucose homeostasis and especially in hepatic glucose production [18]. Thus, beyond their detergent properties, BA modification could trigger endocrine-mediated metabolic disorders. Interestingly, inhibition of intestinal FXR signaling prevents obesity induced by high fat diet and metabolic disease such as insulin resistance and fatty liver [19]. Recently, *Smpd3* (sphingomyelin phosphodiesterase 3), a gene

encoded for the neutral sphingomyelinase 2 (nSMase2) and *Sptlc2* gene, both involved in Cer production, have been identified as FXR target genes [20,21]. These results suggest the existence of a Cer/FXR/BA signaling axis, which could regulate glucose and lipid metabolism.

We investigated the role of *de novo* Cer synthesis in the liver of mice fed with regular chow (RC) or high fat diet (HFD) on energy homeostasis. Using the cre-lox system, we developed a mouse model to decrease Cer *de novo* synthesis in liver by targeting the rate-limiting enzyme subunit, *Sptlc2*, in hepatocytes.

2. Materials and methods

2.1. Animals

All procedures were carried out in accordance with the ethical standards of French and European regulations (European Communities Council Directive, 86/609/EEC). Animal use and procedures were approved by the ethics committee of the University of Paris and by the French ministry of research under the reference #2016040414129137. *Sptlc2*^{lox/lox} mice (kindly given by Dr. Xian-Cheng Jiang, SUNY Downstate Health Sciences University, New York, USA) were crossed with *AlbCre*^{+/-} mice (kindly given by Dr. Catherine Postic, Cochin Institute, Paris, France) to generate mice lacking *Sptlc2* expression in liver (albumin Cre expresses in both hepatocytes and cholangiocytes), *Sptlc2*^{ΔLiv}, or littermate controls, *Sptlc2*^{WTLiv}. Male *Sptlc2*^{WTLiv} and *Sptlc2*^{ΔLiv} were housed in a controlled environment with tap water and *ad libitum* regular food (A04 diet, SAFE, Augy, France) or high fat diet (HF260 diet, SAFE, Augy, France) starting at 8 weeks of age. Mice were maintained on a 12-h light/12-h dark cycle and cages were enriched with tunnels. Number of mice and suffering were minimized in accordance with the 3Rs.

2.2. Metabolic phenotyping

All the protocols used for metabolic phenotyping (body mass composition and metabolic tests) are described in the supplementary methods.

2.3. GW4869 treatment

Transgenic mice (*Sptlc2*^{ΔLiv}) and littermate controls were orally treated at 45 day-old with a selective inhibitor of nSMase 2, GW4869 (catalog n°D1692, SIGMA-ALDRICH, Saint-Louis, MO, USA) in corn oil + DMSO 1 % (vehicle) at 15 mg/kg/day. After the treatment, sphingomyelin measurement was performed on primary hepatocytes to confirm the increase in sphingomyelin content.

2.4. Energy content of feces by bomb calorimeter

Feces were collected every 24 h during one week, dried to constant weight (0.001 g) at 60 °C, and energy content of dried feces (kJ/g) was analyzed for each individual mouse using a bomb calorimeter (IKA C200, Staufen, Germany).

2.5. RNA and protein analysis

Western blot analysis, liver histology for immunohistochemistry or

staining, RNA extraction, cDNA synthesis and real-time PCR were performed using standard protocols already described previously [22,23]. Detailed procedure with a list of the primer sequences can be found in the supplementary methods.

2.6. Quantification of phosphorylated (Ser473) Akt and total Akt

Protein extraction was carried out from liver, adipose tissue and muscle following the same protocol as was used for western blot analysis. Quantitative determination of phospho-Akt (Ser473) and total Akt was assessed by a Meso Scale Discovery (MSD, Kenilworth, NJ, USA) multiplex electrochemiluminescence immunoassay system (Phospho (Ser473)/Total Akt Whole Cell Lysate Kit, catalog n° K15100D) according to manufacturer's instructions.

2.7. Biochemical analyses

Liver triglycerides were measured using triglyceride determination kit from Sigma (catalog n°TR0100, SIGMA-ALDRICH, Saint-Louis, MO, USA) according to the manufacturer's instructions. Liver glycogen content was measured using amyloglucosidase enzyme (catalog n°A7095, SIGMA-ALDRICH, Saint-Louis, MO, USA) assay according to Roehrig and Allred method [24]. Glucose was then determined using Glucose GOD-PAP kit (catalog n°87,109, BIOLABO, Maizy, France). Plasma concentrations of alanine amino-transferase (ALAT), aspartate amino-transferase (ASAT), direct bilirubin and alkaline phosphatase were determined using an automated Monarch device (CEFI, IFR02, Paris, France) as described previously [25].

2.8. Isolation of primary mouse hepatocytes

Hepatocytes from 45 day-old *Sptlc2*^{WTLiv} and *Sptlc2*^{ΔLiv} mice were isolated as previously described [26]. Procedure for glucose production measurement from primary hepatocytes is described in supplementary methods.

2.9. G6pase activity assay and liver G6P content measurement

G6Pase activity was assayed in liver homogenates for 10 min at 30 °C at pH 7.3 in the presence of a saturating glucose-6-phosphate concentration of 20 mM as described [27]. Hepatic glucose-6-phosphatase (G6P) determinations were carried out as previously described [28].

2.10. Quantification of sphingolipids

LC-MS/MS technic was used for sphingolipids quantification. Detailed procedure can be found in the supplementary methods.

2.11. Bile acids measurements

BA measurements were performed on mouse gallbladder bile, plasma, liver and feces by high-performance liquid chromatography-tandem mass spectrometry as described in [29,30]. The hydrophobicity index takes into account the retention time of different BA on a C18 column with a gradient of methanol; the LCA has the highest retention time, the TUDCA-3S has the lowest.

2.12. Gut microbiota analysis

We analyzed gut microbiota in *Sptlc2*^{WTLiv} and *Sptlc2*^{ΔLiv} mice under HFD, by collecting the caecum content at sacrifice and performing 16S ribosomal RNA sequencing. Detailed procedure can be found in the supplementary methods.

2.13. Statistical analysis

Data are expressed as means ± SEM. Statistical analysis was performed using Student's *t*-test, Mann-Whitney *U* test or two-way ANOVA followed by two-by-two comparisons using Bonferroni's *post hoc* test (GRAPHPAD Prism 6 Software, La Jolla, CA, USA). Differences were considered significant at *p* < 0.05.

3. Results

3.1. Genetic deletion of *Sptlc2* in liver increases selective ceramide content in the liver but decreases sphingomyelin content associated with an up-regulation of *nSmase2/Smpd3*

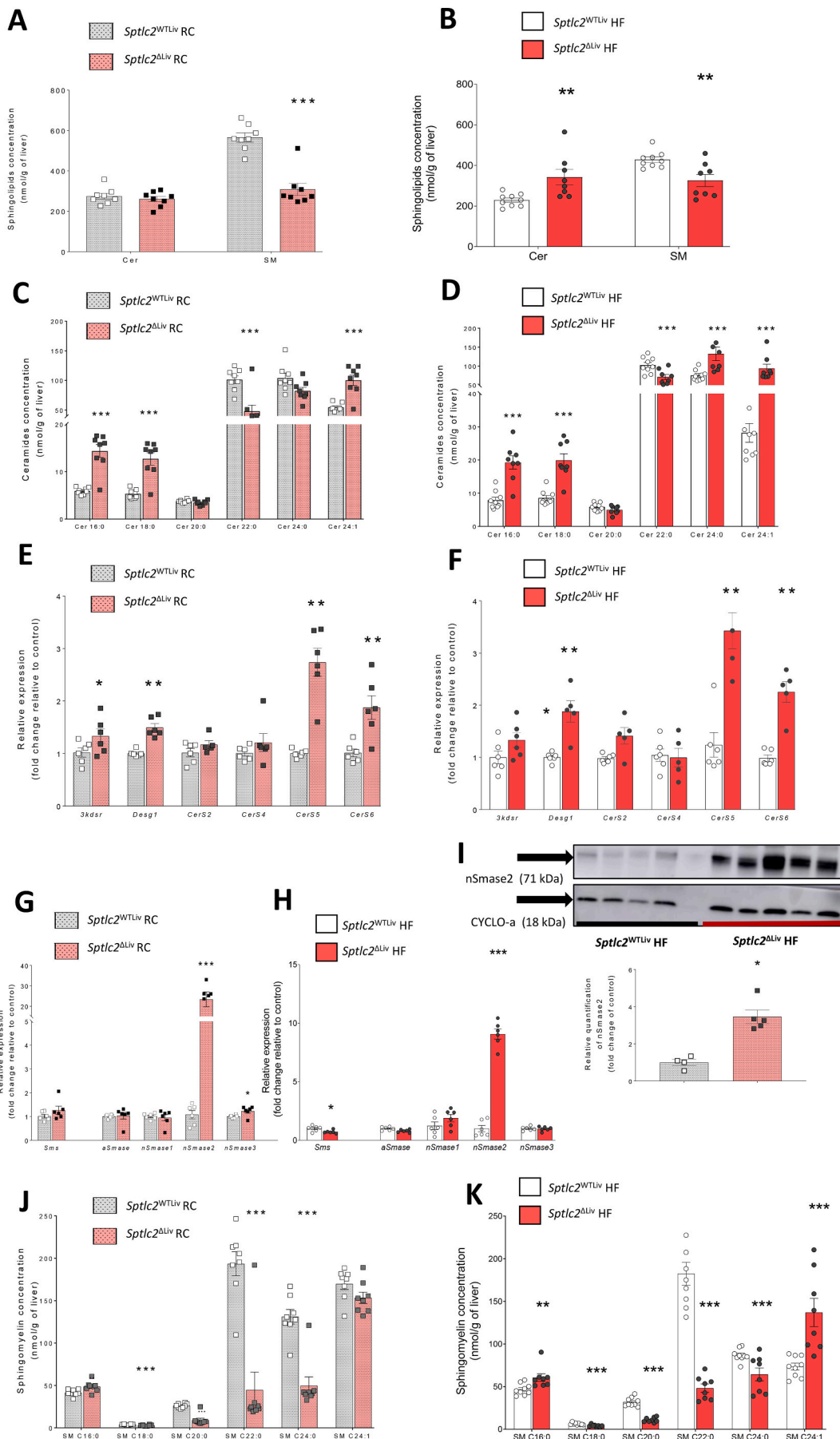
Sptlc2^{lox/lox} mice were crossed with heterozygous mice, which expressed the protein Cre driven by the albumin promoter (Fig.S1A). *Sptlc2* hepatic mRNA level was reduced to 60 % of wild type (WT) level both in *Sptlc2*^{ΔLiv} mice fed with RC or HFD (Fig.S1B), consistent with the fact that hepatocytes (main albumin producers) represent about 70 % of all liver cells [31]. Enzymatic SPT2 activity was accordingly reduced to 60 % of controls (Fig. S1C). Surprisingly, in our genetic model, *Sptlc2* deficiency does not induce Cer reduction in liver of RC mice (Fig. 1A) and even elicits hepatic Cer accumulation in HFD fed mice (Fig. 1B). Moreover, *Sptlc2* deletion modifies hepatic Cer species distribution. Thus, we showed C16:0-Cer, C18:0-Cer and C24:1-Cer accumulation and C22:0-Cer reduction in the liver of mutant mice (Fig. 1C-D). Quantification of Cer in isolated hepatocytes from *Sptlc2*^{ΔLiv} mice and their littermate controls confirmed the increase in C16:0-Cer and the decrease in C22:0-Cer (Fig. S1C). Interestingly, *CerS5* and *CerS6*, which catalyze C16:0-Cer and C18:0-Cer synthesis were up regulated in *Sptlc2*^{ΔLiv} mice liver upon RC and HFD (Fig. 1E-F). Please refer to Fig. S1D for ceramide synthesis pathways scheme.

We measured a reduction in SM content in *Sptlc2*^{ΔLiv} mice liver, under both diets (Fig. 1A-B). These results are also confirmed in primary hepatocytes from RC mice (Fig.S1E). These data suggest that the SMase pathway is over-activated to produce Cer through the hydrolysis of sphingomyelin. In line, we measured a dramatic increase in neutral sphingomyelinase 2 (*nSmase2*) mRNA level, which is specifically expressed at plasma membrane, in the liver of KD mice, independently of the diet (Fig. 1G-H). Moreover, up-regulation of *nSmase2* protein levels was also detected by western blot in the liver of RC *Sptlc2*^{ΔLiv} mice (Fig. 1I). The analysis of SM species distribution reveals that the modification of hepatic SM profile is similar to the one observed for Cer species (i.e increase of C16:0-SM and decrease of C22:0-SM) (Fig. 1J-K, Fig. S1F) suggesting a remodeling of Cer species profile due to *CerS5* and *CerS6* up-regulation. Of note, Cer and SM concentration in the plasma were found to be increased in mice lacking *Sptlc2* as compared with WT. Then, hepatic Cer and especially hepatic SM, substrate of *nSmase2*, could be provided by plasma sphingolipids (Fig. S2). Cer and SM contents have been also measured in epididymal adipose tissue, and showed a non-significant trend towards increased SM in the adipose tissue of *Sptlc2*^{ΔLiv} mice (data not shown).

Overall, these data suggest a compensatory mechanism through the SMase pathway to maintain an elevated Cer content in the liver despite the inhibition of *de novo* synthesis pathway.

3.2. *Sptlc2* deficiency in liver impairs bile acid homeostasis leading to a defect in lipid absorption and resistance against obesity induced by high fat diet

We measured BA composition and concentration in the gallbladder bile, liver, ileum and plasma and showed that *Sptlc2*^{ΔLiv} compared to WT mice exhibited substantially elevated BA concentrations in these compartments (Fig. 2A, Fig. S3A), consistent with the reduction of bile flow (i.e. cholestasis) described in prior studies [32]. Moreover, we showed in this study that BA composition was strongly modified between the two



(caption on next page)

Fig. 1. *Sptlc2* deficiency in liver modulates SM/Cer balance and induces *nSmase2* overexpression.

(A–B) Quantification of SM and Cer content in the liver of RC and HFD fed mice. (C–D) Ceramide species distribution according to acyl-chain length in RC and HFD fed mice livers. Relative expression of genes involved in *de novo* ceramides synthesis (E–F) and sphingomyelinase pathway (G–H) in *Sptlc2*^{ΔLiv} mice liver relative to littermate controls upon RC or HFD. (I) Western blot analyses and quantification of *nSmase2* and Cyclo-a in RC fed mice liver. (J–K) SM species distribution in RC and HFD fed mice liver. Analysis were performed in 4 month-old mice and HFD mice were fed with HFD for 2 months starting at 2 month-old; error bars represents SEM; *n* = 4–10 mice per groups; **p* < 0.05, ***p* < 0.01, ****p* < 0.001 via Mann-Whitney *U* test.

groups of mice, independently of the diet (Fig. 2B, Fig. S3B). A dramatic increase in β-MCA, the dominant form of muricholic acid and in its preponderant conjugated form, tauro-muricholic acid (T-MCA) was observed in mutant mice (Fig. 2B–C, Fig. S3B–C) while secondary BA, most hydrophobic, were almost absent. Except in the plasma, cholic acid (CA) concentration was also reduced in enterohepatic tissues in *Sptlc2*^{ΔLiv} mice (Fig. 2B, Fig. S3B). In line with these data, the hydrophobicity index of the BA pool was decreased in liver, gallbladder bile, ileum and plasma from *Sptlc2*^{ΔLiv} as compared with WT mice (Fig. 2D, Fig. S3D). We measured serum C4 levels, which reflect BA synthesis, and showed higher levels in *Sptlc2*^{ΔLiv} mice whatever the diet (Fig. S3E). Elevated plasma BA were associated with severe jaundice in mutant mice, along with moderate cytolysis and strong elevation of alkaline phosphatase and bilirubin (Fig. 2E and Table 1), consistent with cholestasis. These changes in BA homeostasis were accompanied with altered gut microbiota profile, consistent with the fact that BA and gut microbiota are in close interrelationship as microbiota converts primary BA into secondary BA. At the phylum level, we evidenced increased Bacteroidetes and decreased Proteobacteria in *Sptlc2*^{ΔLiv} mice (Fig. S6A), while at the family level, *Sptlc2*^{ΔLiv} mice microbiome showed the presence of bacteria almost absent in the controls such as Sutterellaceae and Erysipelotrichaceae (Fig. S6B).

Interestingly in this cholestatic context, mutant mice exhibited disrupted localization of cytokeratin 19 (Ck19) immunostaining (a marker of cholangiocytes) (Fig. 2F), suggesting that cholangiocyte injury occurred in these mice and may contribute to bile flow impairment, *i.e.* to cholestasis. Furthermore, we measured main BA transporters and BA synthesis enzymes mRNAs. Interestingly, *Cyp8b1* (CA synthesis) and *Cyp27a1* (alternative pathway) mRNAs were both reduced in *Sptlc2*^{ΔLiv} mice liver (Fig. 2G). Together with a strong decrease in mRNA *Ntcp* level (hepatocyte basolateral uptake BA transporter) (Fig. 2H), these variations could be part of an adaptive response to BA accumulation in hepatocytes as already well described [33]. In addition, consistent with the dramatic increase in T-MCA, a BA reported as an FXR antagonist [17], a significantly decreased expression in the *Fxr* target genes *Shp* and *Fgf15* was observed in ileum and liver from *Sptlc2*^{ΔLiv} as compared with WT mice (Fig. 2I–J). Thus, *Sptlc2* deficiency in liver leads to profound changes in BA synthesis and transport together with a decreased FXR target genes expression in both ileum and liver.

As modifications of BA composition, synthesis and transport could impair lipid absorption [34], we fed *Sptlc2*^{ΔLiv} mice and their littermate controls with HFD for 8 weeks in an attempt to induce obesity. Interestingly we measured an increased energetic density of KD mice feces (Fig. 3A) associated with impaired triglyceride absorption, as revealed by reduced plasma triglycerides in *Sptlc2*^{ΔLiv} as compared with WT mice up to 6 h after an oral olive oil charge (Fig. 3B). In line with these data, *Sptlc2* mutant mice upon HFD (starting from week 4) gained significantly less body weight than control animals, despite similar food intake (Fig. 3C–D). Of note, RC fed *Sptlc2*^{ΔLiv} and WT mice exhibited similar body weight gain (Fig. 3E). However, mass composition analysis revealed a decreased fat mass in KD compared to WT mice upon both RC and HFD (Fig. 3F). Altogether, these results suggest that *Sptlc2*^{ΔLiv} mice exhibited a defect in lipid absorption leading to body weight gain resistance upon HFD.

3.3. Genetic deletion of *Sptlc2* in liver impairs hepatic glucose production and storage in an insulin-independent manner

The liver is at the core of glucose metabolism: it produces glucose from the breakdown of glycogen, or through gluconeogenesis from lactate, pyruvate, glycerol and amino acids [35]. Interestingly, decreased level of hepatic *Sptlc2* prevents glucose intolerance in mice challenged with HFD (Fig. 4A–C). This could be due, in part, to the lack of weight gain upon HFD in *Sptlc2* KD mice (see above). However, *de novo* glucose production from pyruvate (Fig. 4D–F) and glycerol (Fig. 4G–I) were decreased in KD mice either fed with HFD or RC. This observed *in vivo* defect in hepatic glucose production is supported by glucose production measurements on isolated primary hepatocytes (Fig. S4A–B). Two and three hours after hepatocyte stimulation induced by medium without glucose containing pyruvate and glycerol, we detected a tendency of a reduced glucose production in isolated hepatocytes from *Sptlc2*^{ΔLiv} mice. Indeed, hepatic *Sptlc2* deficiency decreases glucose-6-phosphatase (*G6pase*) and pyruvate carboxylase (*Pc*) expression levels (Fig. 4J). Furthermore, *G6pase* activity and glucose-6-phosphate (G6P) content were decreased in mutant mice liver (Fig. 4K–L).

Another series of mice were orally treated with a *nSmase2* inhibitor, GW4869 (Fig. 4M–P). *Sptlc2*^{ΔLiv} treated with GW4869 (15/mg/kg/day) displayed no significant difference for AUCs of PTT and GlyTT compared with WT, treated or not (Fig. 4 O–P), suggesting a normalization of their hepatic glucose production. We checked *ex vivo*, on isolated hepatocytes, the effect of GW4869 treatment on SM hydrolysis and thus, SM concentration, and measured as expected an overall increase in SM concentration (*P* = 0.024, *n* = 6, not shown) consistent with decreased sphingomyelinase activity.

In order to evaluate the role of insulin on glucose homeostasis in our transgenic model, we measured insulin secretion during the course of glucose tolerance test and insulin sensitivity. Hepatic deletion of *Sptlc2* did not impair insulin secretion or systemic insulin sensitivity (Fig. 5A–C). Moreover, as expected based on C16:0-Cer and C18:0-Cer accumulation in the liver, activation by phosphorylation on serine 473 of Akt/Pkb (protein kinase B), is reduced in the liver of mutant mice (Fig. 5D–F). Thus, systemic insulin sensitivity is likely compensated by an enhanced Akt/Pkb phosphorylation in the muscle (Extensor Digitorum Longus, EDL). In addition, reduced liver glycogen content was also observed in *Sptlc2*^{ΔLiv} mice at fed state or at 5 h fasted state, as compared with WT mice (Fig. 5G) and we also measured in mutant mice a lower glycemia after 6 h fast (Fig. S4 C–D). Glycogen production in the liver is also controlled by insulin, thus these results are in line with hepatic insulin resistance observed in *Sptlc2*^{ΔLiv} mice. Altogether, these results demonstrated that hepatic *Sptlc2* deficiency impairs hepatic glucose production in an insulin-independent manner.

3.4. Hepatic *Sptlc2* deficiency leads to liver injury and proliferation, inflammation and fibrosis

Based on our data, we next asked whether modulating Cer levels could lead to liver damage. Sirius red and H&E liver section staining revealed that *Sptlc2*^{ΔLiv} mice exhibited necrosis, inflammatory infiltration and fibrosis, increasing progressively with age (Fig. 6A). At 20 days, bile infarcts (*i.e.* necrotic cell clusters characteristic of BA overload), were observed in livers from *Sptlc2*^{ΔLiv} mice but not in WT, without any significant fibrosis. At 45 days and even more at 120 days, patent fibrosis was observed, with both perisinusoidal and porto-portal accumulation

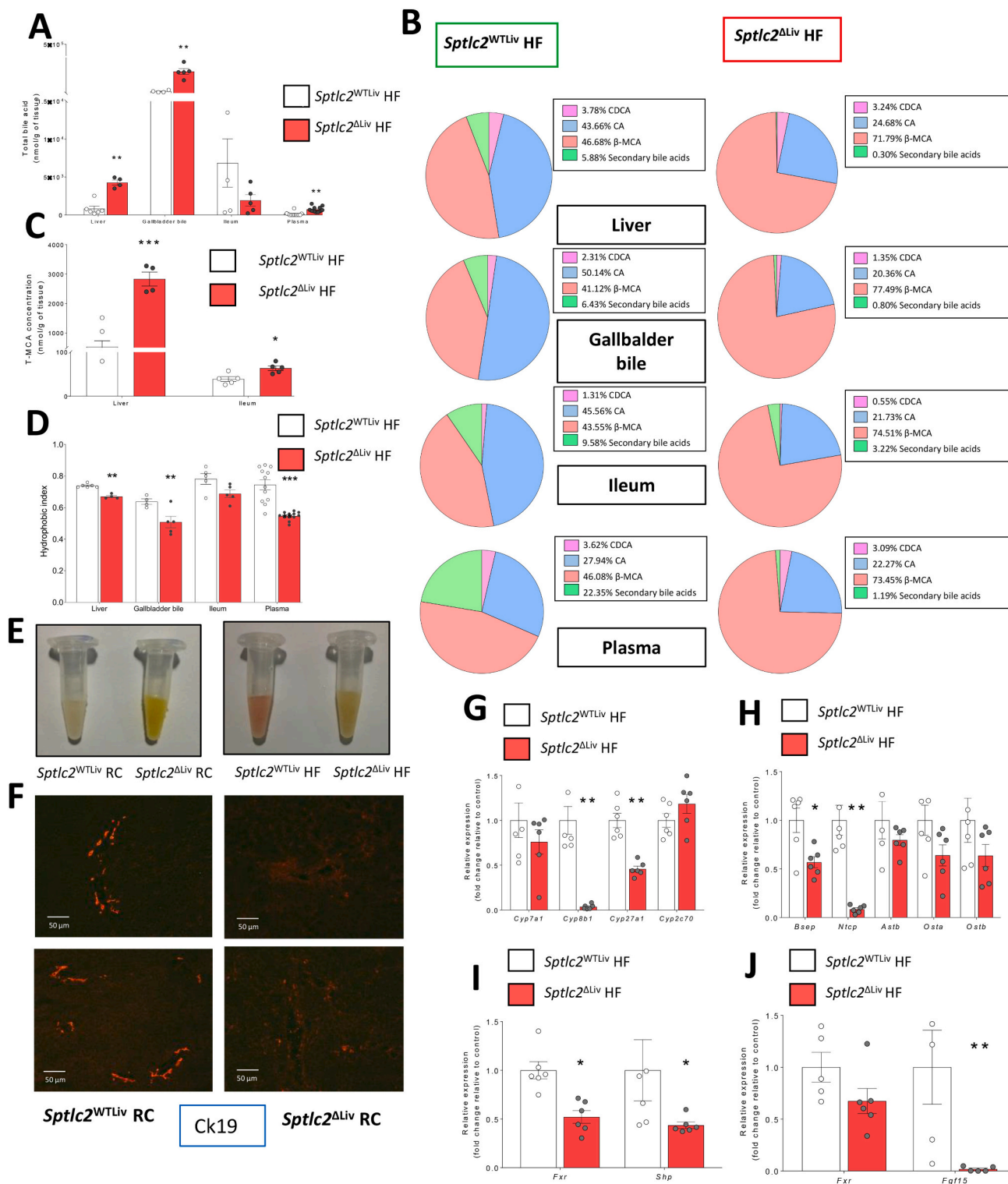


Fig. 2. Genetic deletion of *Sptlc2* in hepatocytes impairs BA composition and metabolism.

(A-B) Total bile acids content and BA composition in liver, gallbladder bile, ileum and plasma of HFD fed mutant and control mice. (C) Tauro-muricholic acid concentration in liver and ileum. (D) Hydrophobicity index of bile acids pool contained in liver, gallbladder bile, ileum and plasma of HFD fed mice. (E) Photograph of representative plasma samples from *Sptlc2*^{WT}Liv or control mice upon RC or HFD. (F) Representative immunofluorescence image showing Ck19 in liver sections of RC fed 3-month-old mice (G) Relative expression of main enzymes involved in bile acids synthesis in liver (G) and bile acids transporters in the liver (*Bsep*, *Ntcp*) or terminal ileum (*Astb*, *Osta*/ β) (H) of HFD fed mice, data are expressed in fold change relative to control. (I-J) Relative expression of *Fxr* and its target gene in the liver (*Shp*) or terminal ileum (*Fgf15*) of HFD fed mice, data are expressed in fold change relative to control. Analysis was performed in 4 months-old mice and HFD mice were fed with HFD for 2 months starting at 2 month-old; $n = 4-10$ mice per groups; error bars represents SEM; * $p < 0.05$, ** $p < 0.01$, *** $p < 0.001$ via Mann-Whitney *U* test, Student's *t*-test when appropriate or two-way ANOVA followed by two-by-two comparisons using Bonferroni's *post hoc* test.

Table 1

Plasma marker of hepatic cholestasis and liver injury in *Sptlc2*^{WT^{Liv}} HFD fed mice and *Sptlc2*^{Δ^{Liv}} HFD fed mice.

	<i>Sptlc2</i> ^{WT^{Liv}} HF	<i>Sptlc2</i> ^{Δ^{Liv}} HF	p-value (Mann-Whitney U test)
Albumin (g/L)	28.3 ± 0.4189	27.3 ± 0.5795	0.243
ALAT (U/L)	47.6 ± 8.165	167.9 ± 11.99	0,00002 ***
ASAT (U/L)	140.7 ± 26.59	323.5 ± 49.09	0.00001 ***
Direct Bilirubin (umol/L)	0.6 ± 0.1017	15.5 ± 3.929	0.0003 ***
Alkaline Phosphatase (U/L)	42.1 ± 3.247	469.1 ± 57.53	0.0003 ***

Analysis were performed in 4 months-old mice and HFD mice were fed with HFD for 2 months starting at 2 months-old; values are means ± SEM; n = 6 mice per groups; ***p < 0.001 via Student's *t*-test.

of extracellular matrix (ECM). Interestingly, HFD did not appear to exacerbate ECM accumulation in liver, demonstrating strong impact of *Sptlc2* disruption on the setting of liver fibrosis. These results were associated with an increased liver weight without triglyceride accumulation, as compared to the littermate controls (Fig. 6.B-C).

As inflammation, which could be triggered by unbalanced Cer proportions, is known to be associated with liver disorders [36,37], we assessed inflammatory response activation through the presence of granulocyte receptor-1 (*Gr-1*) positive cells in frozen liver tissue sections. In line with H&E staining, as shown in Fig. 6D, inflammatory *Gr1* positive cells were strongly increased in KD mice liver sections as compared with WT. Also, hepatic mRNAs encoding tumor necrosis alpha (*Tnfα*), a proinflammatory cytokine, also involved in apoptosis- and its TNF receptor 1 (*Tnfr-1*), were significantly elevated in mice lacking expression of *Sptlc2* in the liver (Fig. 6E).

Western blot analysis revealed increased cleaved Casp3 content in the liver from HFD-fed *Sptlc2*^{Δ^{Liv}} mice as compared with WT (Fig. 6F-G). Moreover, in *Sptlc2*^{Δ^{Liv}} mice, genes belonging to B-cell lymphoma 2 (*Bcl2*) family (apoptosis regulators), were significantly modulated. *Bcl-2* and *Bcl-2*-associated X protein (*Bax*), respectively anti-apoptotic and pro-apoptotic molecules, were up-regulated, indicating apoptosis deregulation in KD mice upon HFD (Fig. 6H). In agreement with these results, Ki67 immunostaining (a proliferation marker), revealed a dramatic increase of cell proliferation in mutant as compared with WT, demonstrating a high apoptosis/proliferation rate in the liver of mice lacking SPTLC2 (Fig. 6I). Interestingly, this *Sptlc2*^{Δ^{Liv}} phenotype was not associated with any ER stress, since *Gpr78* and *Chop* expression in liver were not affected by *Sptlc2* deficiency (Fig. 6J).

Longitudinal studies revealed, in 20-day-old *Sptlc2*^{Δ^{Liv}} mice, the presence of both bile infarcts on liver sections and altered BA pool composition (i.e increase MCA and decrease secondary BA), without any significant hepatic fibrosis (Fig. S5A). Likewise, we observed a defect in hepatic glucose production in *Sptlc2*^{Δ^{Liv}} mice from 20 days, indicating that gluconeogenesis alteration was not related to hepatic fibrosis development (Fig. S5B). Altogether, these results showed that hepatic *Sptlc2* disruption led to early inflammatory liver injury, with progressive development of liver fibrosis with age, in association with abnormally high rates of apoptosis and proliferation.

4. Discussion

We demonstrate for the first time a potential compensatory mechanism regulating hepatic Cer content from SM hydrolysis, and highlight the role of hepatic SL modulation on the setting of hepatic fibrosis, BA composition changes and hepatic glucose production.

We investigated the role of hepatic Cer *de novo* synthesis in energy homeostasis in mice upon RC or HFD. Interestingly, genetic deletion in liver of *Sptlc2* does not reduce total intrahepatic and plasma Cer level,

and even increases plasma and liver Cer content in HFD fed mice. However, we show a significant decrease of the C22:0-Cer specie in liver, and both C22:0-Cer and C24:0-Cer diminution is evidenced in primary hepatocytes. These Cer species are the most abundant in liver, partially because of the high expression level of *Cers2* involved in C22:0-Cer and C24:0-Cer formation from dihydrosphingosine [38]. Thus, in our model, *Sptlc2* deficiency reduces Cer production from *de novo* synthesis for the benefit of another production pathway. Indeed, nSMase2 mRNA and protein levels are up-regulated in *Sptlc2*^{Δ^{Liv}} mice, suggesting over-activation of the sphingomyelinase pathway at plasma membrane. Our data suggest for the first time to our knowledge a compensatory mechanism to maintain (and even to increase) Cer production through the dramatic up-regulation of nSMase2 expression.

A direct regulatory interaction between SPTLC2 and nSMase2 is unlikely due to different intracellular localization, however the decreased utilization of serine and palmitoyl-CoA (SPTLC2 substrates) could lead to a modulation of nSMase2 activity. Indeed, previous studies showed that nSMase2 was activated by fatty acids and phosphatidylserine [39–41]. In addition, the development of pro-inflammatory environment due to the lack of ceramide *de novo* synthesis could also induce nSMase2 up-regulation [42,43]. Interestingly, nSMase2 expression has been correlated with inflammation in different organs [43–45], and in particular the activation of TNF-R by a ligand as TNF-α has been shown to induce nSMase2 translocation to the plasma membrane and ceramides synthesis [46–48]. These is consistent with the up regulation of both TNF-R and TNF-α expression in *Sptlc2*^{Δ^{Liv}} mice. Although the fine mechanisms leading to an overproduction of Cer remain unclear, these data suggest that Cer are essential components for the cell and that an attempt to alter their *de novo* synthesis would trigger a cellular response to avoid a drop in Cer content, at the expense of SM concentration.

Interestingly, acute reduction of *Sptlc2* expression or activity using adenovirus targeting *Sptlc2* in liver, or pharmacological inhibitors such as myriocin, does not induce Cer accumulation [12,41], in contrast to chronic *Sptlc2* deletion using genetic approach which led to Cer and especially C16:0-Cer increase in liver and adipose tissue [32,49]. In the liver, authors have shown that specific deletion of *Sptlc2* induces SM reduction and Cer accumulation in plasma membrane of hepatocytes, supporting the hypothesis of a compensatory mechanism through over-activation of SM hydrolysis at plasma membrane [32]. Interestingly, *Cers2* null mice display changes in the composition of liver Cer species, which are similar to these highlighted in our transgenic mouse model. In addition, the authors have also demonstrated an up-regulation of *Cers5* and nSMase2 gene expression. These results corroborate the existence of a compensatory mechanism between the different pathways of Cer synthesis in liver [50].

We also observe the up-regulation of *Cers5* and *Cers6*, which allows C16:0-Cer and C18:0-Cer formation from dihydrosphingosine. As neutral SMase 2 is known to preferentially use very long acyl chain SM (reduced in the liver and primary hepatocytes in our model), C16:0-Cer and C18:0-Cer accumulation could result from *Cers5* and *Cers6* up-regulation and their substrates would likely be provided by SM hydrolysis and ceramidase action [51]. Moreover, C16:0-Cer accumulation in liver is consistent with the observed C16:0-SM increase in plasma and suggests C16:0-SM supply from one or several other tissues. This hypothesis suggests the existence of a crosstalk between the different tissues to normalize Cer production. Of note, besides SM transport to the liver by circulating lipoproteins, SM species could be transported by extracellular vesicles [52]. Then, we demonstrated in mutant mice a dramatic increase in hepatic C16:0-Cer and C18-Cer which are well described as apoptotic inducers and inflammation triggers [53]. Taken altogether, our data suggest two distinct pools of Cer (in plasma membrane and endoplasmic reticulum) with likely different cellular functions.

We also show that the modulation of sphingolipid metabolism in liver leads to a strong alteration of liver homeostasis, in particular we

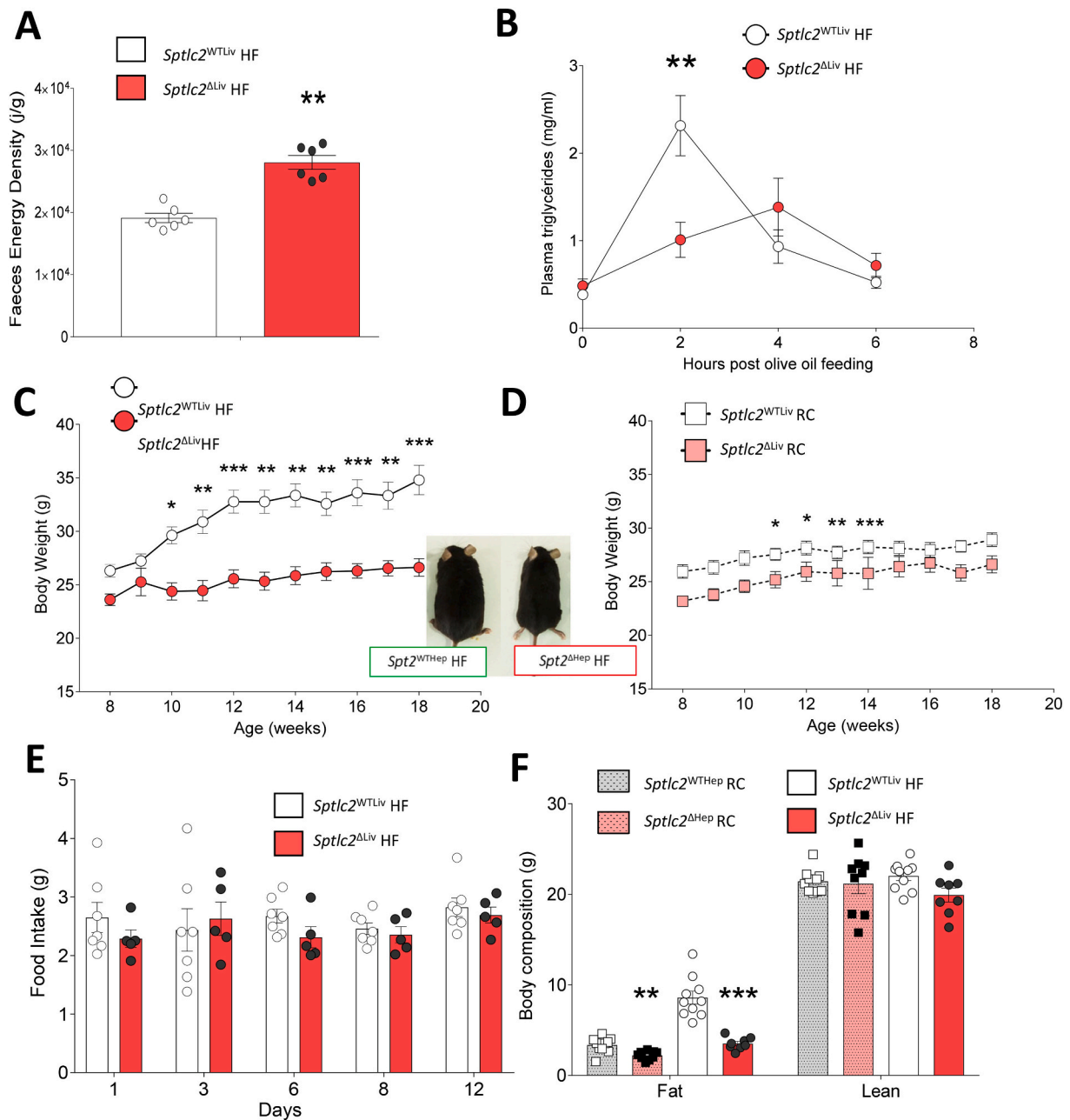


Fig. 3. Genetic deletion of *Sptlc2* in hepatocytes prevents HFD-induced obesity. (A) Energy density of feces collected every 24H of HFD fed mice. (B) Plasma triglycerides measurement after oral olive oil charge in HFD fed mice. (C–D) Body weight change in *Sptlc2*^{ΔLiv} and their littermate controls upon HFD or RC. (E) Time course of food intake in HFD fed mice. (F) Body fat and lean composition, in grams. Analysis were performed in 4 months-old mice and HFD mice were fed with HFD for 2 months starting at 2 month-old; n = 4–10 mice per groups; error bars represents SEM; *p < 0.05, **p < 0.01, ***p < 0.001 via Mann-Whitney U test, Student's *t*-test when appropriate or two-way ANOVA followed by two-by-two comparisons using Bonferroni's *post hoc* test.

evidenced an impairment of BA pool composition associated with a defect in intestinal lipid absorption. Our findings show that primary BA, especially T-MCA, are increased in *Sptlc2*^{ΔLiv} mice and that secondary BA are almost absent. Bile acids and gut microbiota are in close inter-relationship as microbiota converts primary BA into secondary BA, through first the action of Bile salt hydrolases, which allow BA deconjugation. Then, the action of other specific enzymes will end up the conversion of primary BA in secondary BA [54,55]. In addition, BA composition could influence gut microbiome and then BA synthesis, transport or removal impairment could directly induce dysbiosis [56,57].

We accordingly showed strong alteration of *Sptlc2*^{ΔLiv} mice gut

microbiota in accordance with the changes in BA homeostasis. Secondary BA, which are more hydrophobic than primary BA, are essential for intestinal lipid absorption [58]. Accordingly, we measured lower hydrophobic index in BA pool of *Sptlc2*^{ΔLiv} mice leading to lower triglycerides absorption and increased energy density in feces. Taken together, these data are consistent with a full resistance to high-fat induced obesity in *Sptlc2*^{ΔLiv} mice due to altered BA-dependent lipid absorption in the intestine. Of interest, food intake is similar in *Sptlc2*^{ΔLiv} compared to the controls, supporting post-ingestive events rather than nervous perturbation of food behavior.

Sptlc2^{ΔLiv} mice also displayed jaundice as reported [32]. Prior study has also reported alterations in BA transporters localisation and

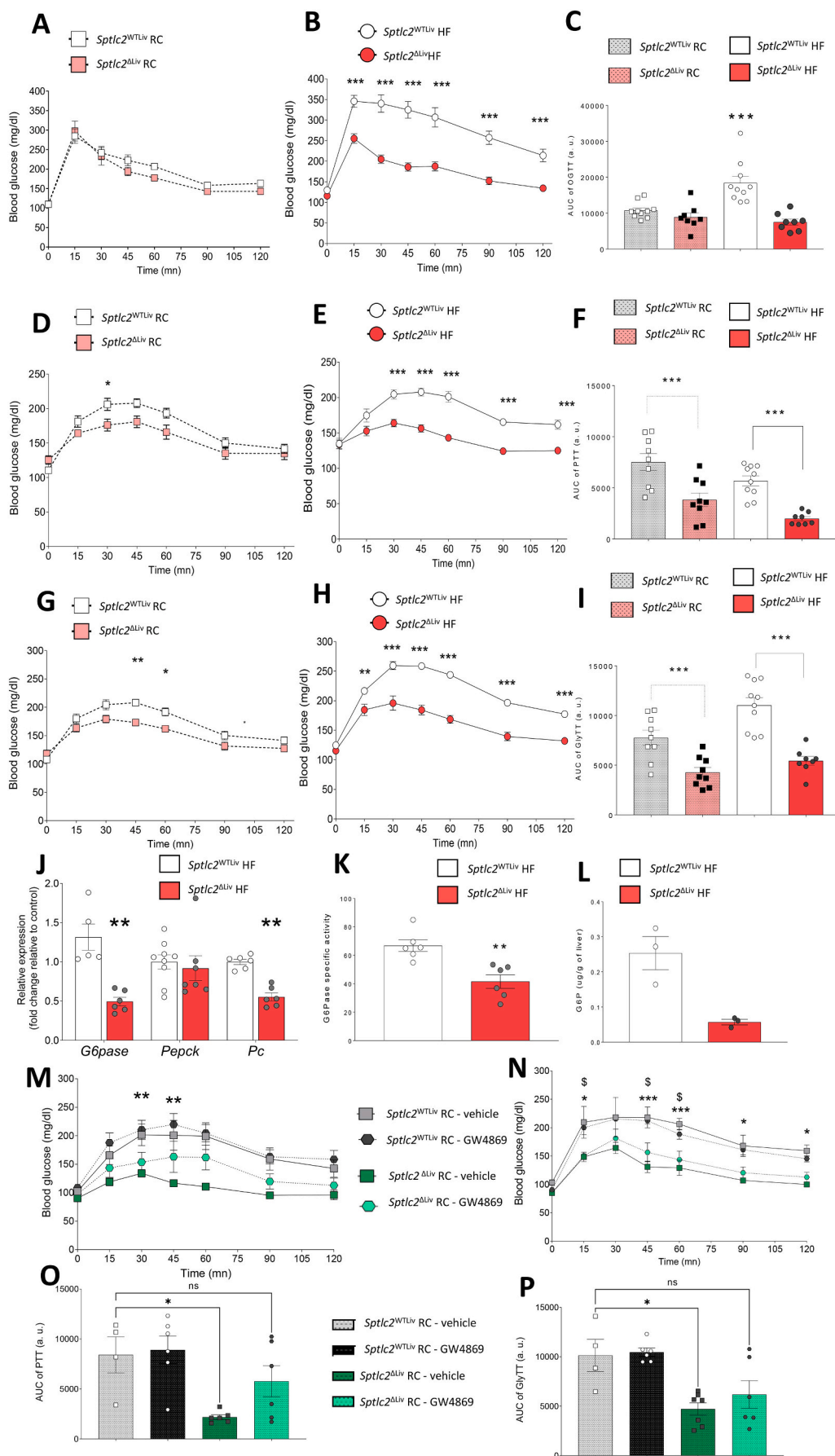


Fig. 4. Genetic deletion of *Sptlc2* in hepatocytes impairs hepatic glucose production and storage OGTT (A-B), PTT (D-E) and GlyTT (G-H) at 1 g/kg performed in RC or HFD fed mice (overnight fasting). (C) Respective areas under the curve for the OGTT (C), PTT (F) and GlyTT (I) in RC or HFD mice. (J) Relative expression of main enzymes involved in gluconeogenesis in liver of HFD fed mice, data are expressed in fold change relative to control. (K-L) G6Pase specific activity and G6P content in liver of HFD fed mice. PTT (M) and GlyTT (N) with respective areas under the curve (O–P) at 1 g/kg performed in RC fed mice orally treated with GW4869 (15 mg/kg/day for 14 days). $n = 3–10$ mice per group; error bars represents SEM; * $p < 0.05$, ** $p < 0.01$, *** $p < 0.001$ via Mann-Whitney *U* test, Student's *t* when appropriate or two-way ANOVA followed by two-by-two comparisons using Bonferroni's *post hoc* test.

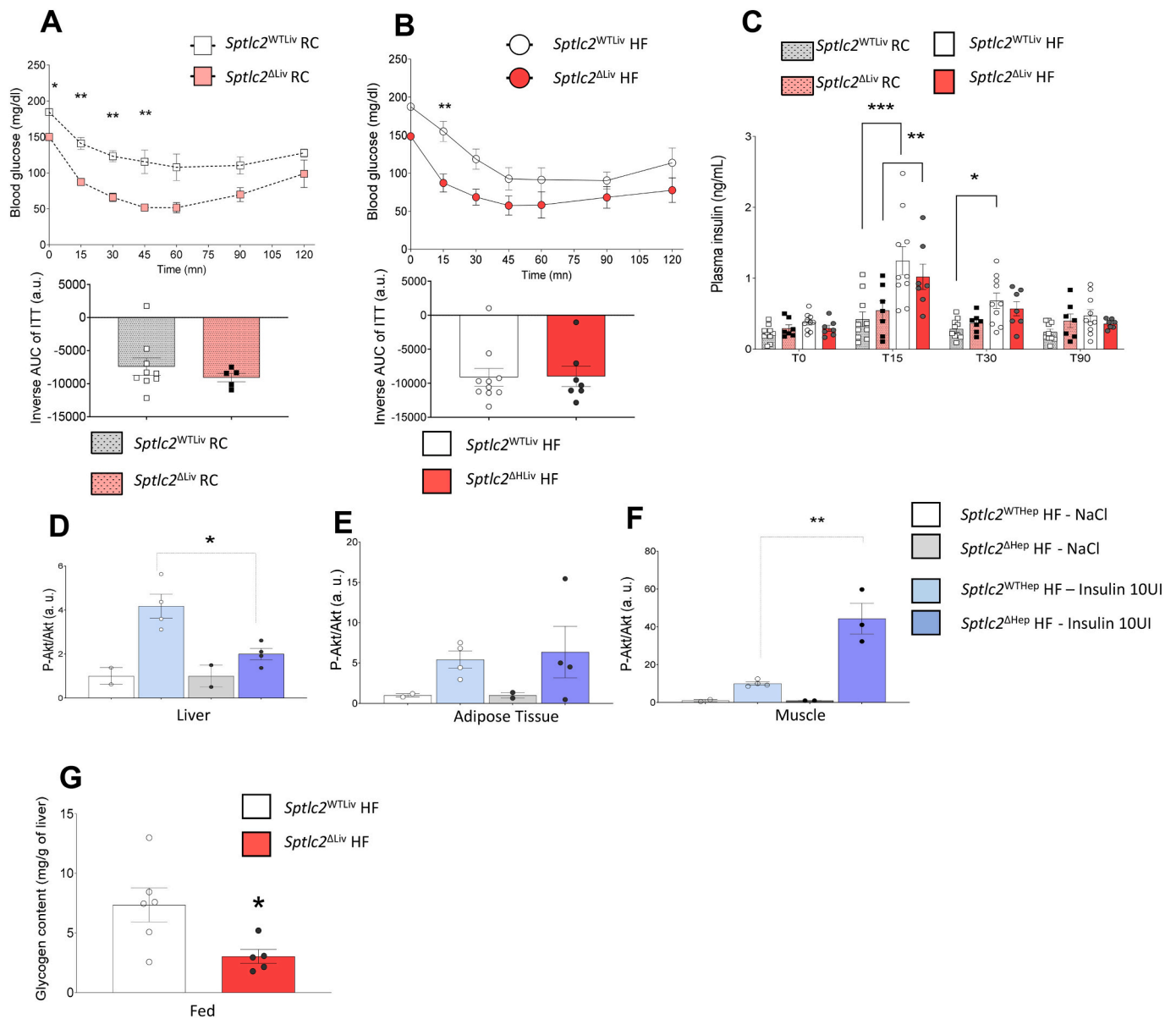


Fig. 5. Impact of hepatic deletion of *Sptlc2* on insulin sensitivity.

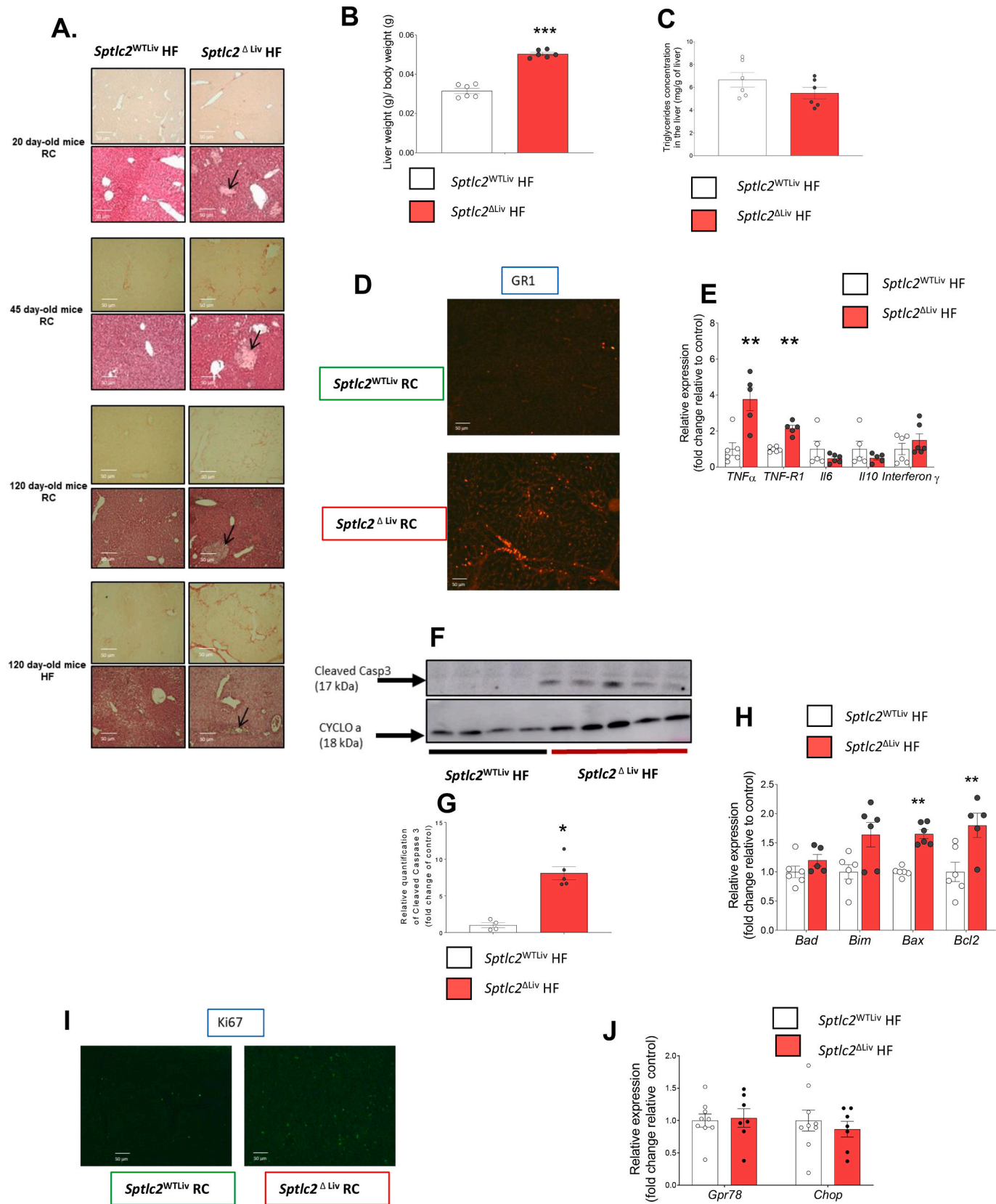
ITT at 0.25 UI/kg (A) or 0.5 UI/kg (B) and inverse areas under the curve performed in RC or HFD fed mice. (C) Plasma insulin secretion during OGTT test of RC or HFD fed mice. (D–F) Phosphorylated Akt (Ser473)/Akt ratio measured in cells lysates from liver, adipose tissue or muscle (extensor digitorum longus) of HFD fed mice stimulated with insulin (10 UI/kg) 30 min before tissue collection. (G) Glycogen content in liver of HFD fed or 5-h-fasting mice. Analysis were performed in 45 day-old mice (for primary hepatocytes collection) or 4 month-old mice and HFD mice were fed with HFD for 2 months starting at 2 month-old. Data are expressed relative to insulin response. Analysis were performed in 4 month-old mice and HFD mice were fed with HFD for 2 months starting at 2 month-old; n = 3–10 mice per groups; error bars represents SEM; **p* < 0.05, ***p* < 0.01, ****p* < 0.001 via Mann-Whitney *U* test, Student's *t* when appropriate or two-way ANOVA followed by two-by-two comparisons using Bonferroni's *post hoc* test.

hepatocyte polarity in liver-specific *Sptlc2* KO mice [32]. Although precise mechanisms of cholestasis development in this model remain to be fully deciphered, our data suggest that, in the lack of SPTLC2 in hepatocytes and cholangiocytes, intrahepatic bile duct cells were disorganized, a feature that likely contributed to bile flow impairment. How cholangiocytes would be injured in these mice remains to be elucidated, but we speculate that the accumulation of pro-inflammatory and proapoptotic Cer observed in *Sptlc2*^{ΔLiv} mice might contribute to biliary epithelial damage. Consistently, Cer have been shown to up-regulate hepatic mRNA expression of lipid metabolism-related genes, inflammation-related (as evidenced in our model) and fibrogenesis-related genes [59].

The nuclear BA receptor FXR is a transcription factor involved in the

regulation of both BA metabolism and glucose homeostasis. There are *in vitro* and *in vivo* evidences that modulation of FXR pathway regulates gluconeogenesis in rodent [60,61]. Consistent with the dramatic increase in T-MCA, a reported FXR antagonist [17], in our mutant mice, we show that genetic deletion of hepatic *Sptlc2* inhibits expression of FXR signaling pathway. Recently, it has been shown that *nSmase2* is a target gene of FXR [20,21]. However, *Fxr* and *nSmase2* vary in opposite ways in our model, suggesting that *sSmase2* upregulation is not linked to FXR but rather to other factors (intracellular substrates, pro-inflammatory environment).

In addition, *Sptlc2*^{ΔLiv} mice have a defect in hepatic glucose production from pyruvate and glycerol, which probably explains, associated with better insulin sensitivity in the muscle, the better glucose



(caption on next page)

Fig. 6. Measurement of biological parameters associated with liver damage, liver fibrosis, inflammation and apoptosis.

(A) Representative images of H&E and sirius red staining. Images were taken in liver sections from 20 day-old RC mice, 45 day-old RC mice, 4 month-old RC mice and 4 month-old HFD mice. Black arrows represent bile infarcts. (B) Ratio liver weight to body weight. (C) Triglycerides content in liver of HFD fed mice. (D) Representative images from immunohistochemical staining for Ly6g/GR1 in liver sections from RC fed mice (3 month-old). (E) mRNA levels of *TNF α* , *TNF-R1*, *Il6*, *Il10* and *Interferon δ* in liver, data are expressed in fold change relative to control. (F-G) Western blot analyses and quantification of cleaved caspase 3 and Cyclo-a in total protein extracted from liver. (H) mRNA levels of *Bad*, *Bim*, *Bax* and *Bcl-2* in liver, data are expressed in fold change relative to control. (I) Representative images from immunohistochemical staining for the marker of proliferation, Ki67, in liver sections from RC fed mice (3 month-old). (J) mRNA levels of *Gpr78* and *Chop* in liver, data are expressed in fold change relative to control. Except for the immunohistochemical staining, analysis were performed in 4 month-old mice and HFD mice were fed with HFD for 2 months starting at 2 month-old; $n = 4-10$ mice per groups; error bars represents SEM; * $p < 0.05$, ** $p < 0.01$, *** $p < 0.001$ via Mann-Whitney U test, Student's t when appropriate or two-way ANOVA followed by two-by-two comparisons using Bonferroni's *post hoc* test.

tolerance under HF. Interestingly, *Sptlc2* ^{Δ Liv} mice treated with a selective nSMase2 inhibitor show a partial normalization of their glucose production in response to pyruvate or glycerol, suggesting that increased SM hydrolysis by nSMase2/Smpd3 upregulation plays a causal role in the hepatic glucose production defect. Of note, 6-hour-fasting glycemia is reduced in *Sptlc2* ^{Δ Liv} mice. These traits are unlikely linked to a liver-specific increase in insulin sensitivity, while Cer, and especially C16:0-Cer and C18:0-Cer, well-known inducers of insulin resistance, accumulate in liver [7]. Consistently, glycogen content is reduced, and phosphorylation of Akt/ protein kinase B (Pkb), a main mediator of insulin anabolic effects is reduced in the liver of mutant mice, while systemic insulin sensitivity seems to be compensated by an enhanced Akt/Pkb phosphorylation in the muscle. Altogether, these results demonstrated that hepatic *Sptlc2* deficiency impaired hepatic glucose production in an insulin independent way.

We also evidenced a previously undescribed age-related effect of SPTLC2 deficiency that favours hepatic fibrogenesis. Although precise mechanisms remain to be investigated, the decreased amount of membrane SM in the lack of hepatic SPTLC2, associated with a reduction of membrane lipids rafts, may favour beta catenin translocation to the nucleus and contribute to the onset of fibrogenesis [32,62]. Moreover, several studies showed that Cer themselves are involved in hepatic fibrogenesis [63]. Interestingly, we demonstrated that the hepatic glucose production defect was already present in 20-day-old *Sptlc2* ^{Δ Liv} mice before the neat onset of fibrosis and altogether our results suggest that hepatic defect in glucose production is independent of fibrosis development over time.

In conclusion, our findings suggest a compensatory mechanism for Cer production in liver, and highlight a link between sphingolipid production, BA metabolism, and glucose production in an insulin-independent way. The BA nuclear receptor FXR, which is involved in both BA homeostasis and energy metabolism, is likely to be at the core of a sphingolipids/BA/neoglucogenesis axis.

CRediT authorship contribution statement

Justine Lallement: Conceptualization, Methodology, Visualization, Investigation, Data curation, Writing- Original draft preparation, Writing - Review & Editing.

Ilyès Raho: Methodology, Visualization, Investigation.

Grégory Merlen: Methodology, Visualization, Investigation.

Dominique Rainteau: Methodology, Visualization, Investigation.

Mikael Croyal: Investigation, Visualization.

Melody Schiffano: Investigation, Visualization.

Nadim Kassis: Investigation, Visualization.

Isabelle Doignon: Investigation, Visualization.

Maud Soty: Investigation, Visualization.

Floriane Lachkar: Investigation, Visualization.

Michel Krempf: Investigation, Visualization.

Matthias Van Hul: Investigation, Visualization.

Patrice D. Cani: Methodology, Visualization, Investigation.

Fabienne Foufelle: Methodology, Visualization, Investigation.

Chloé Amouyal: Methodology, Visualization, Investigation.

Hervé Le Stunff: Methodology, Visualization, Investigation Writing - Review & Editing.

Christophe Magnan: Writing - Review & Editing, Supervision.

Thierry Tordjmann: Writing - Review & Editing, Supervision.

Céline Cruciani-Guglielmacci: Conceptualization, Methodology, Visualization, Investigation, Data curation, Writing- Original draft preparation, Writing - Review & Editing, Supervision.

Declaration of competing interest

P.D.C. is an inventor on patent applications dealing with the use of specific bacteria and components in the treatment of different diseases. P.D.C. was co-founder of The Akkermansia Company SA and Enterosys. The other authors declare no competing interests.

Data availability

Data will be made available on request.

Acknowledgments

We acknowledge the technical platform Functional and Physiological Exploration platform (FPE) for body composition analysis (Université de Paris, BFA, UMR 8251 CNRS, Paris, France), the animal core facility “Buffon” of the University de Paris, Institut Jacques Monod, especially Laëtitia Pontoizeau, for animal husbandry and breeding.

We also acknowledge Dr. Frédéric Preitner and Anabela Rebelo Pimentel Da Costa from the Mouse Metabolic Facility in Center for Integrative genomics, (University of Lausanne, Lausanne, Switzerland) for measurement of energy content in feces; Nicolas Sorhaindo from biochemical analyses facility in Inflammation research center, (Université de Paris, UMR 1149 Inserm, ERL CNRS 8252, Paris, France) for plasma biochemical analyses and Hermine Kakanakou and Sylvie Le Marchand from the genotyping and biochemical facility, Cordeliers research center, (Sorbonne Université, Paris, France) for mouse genotyping. We are grateful to the “Biogenouest Corsaire” core facility for mass spectrometry analyses and the department of pathological anatomy and cytology in Bicêtre Hospital (Le Kremlin-Bicêtre, France) for paraffin-embedded tissues, red sirius and H&E coloration.

We also acknowledge Amandine Gautier-Stein from Université Claude Bernard Lyon 1, (Université de Lyon, INSERM UMR—S1213, Lyon, France) for her scientific advice and protocols.

Funding

This project has received funding from the Innovative Medicines Initiative 2 Joint Undertaking under grant agreement No 115881 (RHAPSODY). This Joint Undertaking receives support from the European Union's Horizon 2020 research and innovation program and EFPIA. This study has also received funding from EUR G.E.N.E project (ANR-17-EURE-0013) and is part of the idEx project #ANR-18-IDEX-0001 of the Université de Paris, both funded by the French government under its Programme d'Investissements d'Avenir. P.D.C. is research director at FRS-FNRS (Fonds de la Recherche Scientifique) and recipient of grants from FNRS (FRFS-WELBIO: WELBIO-CR-2022A-02 and EOS: program no. 40007505).

Appendix A. Supplementary data

Supplementary data to this article can be found online at <https://doi.org/10.1016/j.bbalip.2023.159333>.

References

- [1] B. Chaurasia, S.A. Summers, Ceramides – lipotoxic inducers of metabolic disorders, *Trends Endocrinol. Metab.* 26 (2015) 538–550.
- [2] V. Poytout, R.P. Robertson, Glucolipotoxicity: fuel excess and beta-cell dysfunction, *Endocr. Rev.* 29 (2008) 351–366.
- [3] E. Hajdúch, F. Lachkar, P. Ferré, F. Foufelle, Roles of ceramides in non-alcoholic fatty liver disease, *J. Clin. Med.* 10 (2021) 792.
- [4] T. Hornemann, Y. Wei, A. von Eckardstein, Is the mammalian serine palmitoyltransferase a high-molecular-mass complex? *Biochem. J.* 405 (2007) 157–164.
- [5] N. Insausti-Urkiá, E. Solsona-Vilarrasa, C. García-Ruiz, J.C. Fernández-Checa, Sphingomyelinases and liver diseases, *Biomolecules* 10 (2020), E1497.
- [6] K. Kitatani, J. Idkowiak-Baldys, Y.A. Hannun, The sphingolipid salvage pathway in ceramide metabolism and signaling, *Cell. Signal.* 20 (2008) 1010–1018.
- [7] B.W. Wattenberg, The long and the short of ceramides, *J. Biol. Chem.* 293 (2018) 9922–9923.
- [8] Y. Pewzner-Jung, et al., A critical role for ceramide synthase 2 in liver homeostasis: II. insights into molecular changes leading to hepatopathy, *J. Biol. Chem.* 285 (2010) 10911–10923.
- [9] Y.A. Hannun, L.M. Obeid, Many ceramides, *J. Biol. Chem.* 286 (2011) 27855–27862.
- [10] S. Raichur, et al., CerS2 haploinsufficiency inhibits β -oxidation and confers susceptibility to diet-induced steatohepatitis and insulin resistance, *Cell Metab.* 20 (2014) 687–695.
- [11] A.L. Birkenfeld, G.I. Shulman, Nonalcoholic fatty liver disease, hepatic insulin resistance, and type 2 diabetes, *Hepatology* 59 (2014) 713–723.
- [12] W.L. Holland, et al., Inhibition of ceramide synthesis ameliorates glucocorticoid-, saturated-fat-, and obesity-induced insulin resistance, *Cell Metab.* 5 (2007) 167–179.
- [13] M. Jiang, C. Li, Q. Liu, A. Wang, M. Lei, Inhibiting ceramide synthesis attenuates hepatic steatosis and fibrosis in rats with non-alcoholic fatty liver disease, *Front. Endocrinol.* 10 (2019).
- [14] M. Makishima, et al., Identification of a nuclear receptor for bile acids, *Science* 284 (1999) 1362–1365.
- [15] E. Studer, et al., Conjugated bile acids activate the sphingosine-1-phosphate receptor 2 in primary rodent hepatocytes, *Hepatology* 55 (2012) 267–276.
- [16] B. Goodwin, et al., A regulatory cascade of the nuclear receptors FXR, SHP-1, and LRH-1 represses bile acid biosynthesis, *Mol. Cell* 6 (2000) 517–526.
- [17] S.I. Sayin, et al., Gut microbiota regulates bile acid metabolism by reducing the levels of tauro-beta-muricholic acid, a naturally occurring FXR antagonist, *Cell Metab.* 17 (2013) 225–235.
- [18] L. Sun, J. Cai, F.J. Gonzalez, The role of farnesoid X receptor in metabolic diseases, and gastrointestinal and liver cancer, *Nat. Rev. Gastroenterol. Hepatol.* 18 (2021) 335–347.
- [19] C. Jiang, et al., Intestine-selective farnesoid X receptor inhibition improves obesity-related metabolic dysfunction, *Nat. Commun.* 6 (2015) 10166.
- [20] C. Xie, et al., An Intestinal Farnesoid X Receptor–Ceramide Signaling Axis Modulates Hepatic Gluconeogenesis in Mice, *Diabetes* 66 (2017) 613–626.
- [21] Q. Wu, et al., Suppressing the intestinal farnesoid X receptor/sphingomyelin phosphodiesterase 3 axis decreases atherosclerosis, *J. Clin. Invest.* 131 (2021).
- [22] J. Véret, et al., Ceramide synthase 4 and de novo production of ceramides with specific N-acyl chain lengths are involved in glucolipotoxicity-induced apoptosis of INS-1 β -cells, *Biochem. J.* 438 (2011) 177–189.
- [23] M. Campana, et al., Inhibition of central de novo ceramide synthesis restores insulin signaling in hypothalamus and enhances β -cell function of obese Zucker rats, *Mol. Metab.* 8 (2018) 23–36.
- [24] K.L. Roehrig, J.B. Alred, Direct enzymatic procedure for the determination of liver glycogen, *Anal. Biochem.* 58 (1974) 414–421.
- [25] B. Viollet, et al., The AMP-activated protein kinase α 2 catalytic subunit controls whole-body insulin sensitivity, *J. Clin. Invest.* 111 (2003) 91–98.
- [26] A. Besnard, et al., The P2X4 purinergic receptor impacts liver regeneration after partial hepatectomy in mice through the regulation of biliary homeostasis, *Hepatology* 64 (2016) 941–953.
- [27] G. Mithieux, et al., Induction of control genes in intestinal gluconeogenesis is sequential during fasting and maximal in diabetes, *Am. J. Physiol. Endocrinol. Metab.* 286 (2004) E370–E375.
- [28] A. Penhoat, L. Fayard, A. Stefanutti, G. Mithieux, F. Rajas, Intestinal gluconeogenesis is crucial to maintain a physiological fasting glycemia in the absence of hepatic glucose production in mice, *Metabolism* 63 (2014) 104–111.
- [29] N. Péan, et al., The receptor TGR5 protects the liver from bile acid overload during liver regeneration in mice, *Hepatology* 58 (2013) 1451–1460.
- [30] V. Bidault-Jourdainne, et al., TGR5 controls bile acid composition and gallbladder function to protect the liver from bile acid overload, *JHEP Rep. Innov. Hepatol.* 3 (2021), 100214.
- [31] K. Si-Tayeb, F.P. Lemaigre, S.A. Duncan, Organogenesis and development of the liver, *Dev. Cell* 18 (2010) 175–189.
- [32] Z. Li, et al., Liver Serine Palmitoyltransferase (SPT) activity deficiency in early life impairs adherens junctions and promotes tumorigenesis, *Hepatology* 64 (2016) 2089–2102.
- [33] G. Zollner, et al., Hepatobiliary transporter expression in percutaneous liver biopsies of patients with cholestatic liver diseases, *Hepatology* 33 (2001) 633–646.
- [34] P.R. Holt, The roles of bile acids during the process of normal fat and cholesterol absorption, *Arch. Intern. Med.* 130 (1972) 574–583.
- [35] L. Rui, Energy metabolism in the liver, *Compr. Physiol.* 4 (2014) 177–197.
- [36] E. Seki, R.F. Schwabe, Hepatic inflammation and fibrosis: functional links and key pathways, *Hepatology* 61 (2015) 1066–1079.
- [37] Y. Koyama, D.A. Brenner, Liver inflammation and fibrosis, *J. Clin. Invest.* 127 (2017) 55–64.
- [38] E.L. Laviad, et al., Characterization of ceramide synthase 2: tissue distribution, substrate specificity, and inhibition by sphingosine 1-phosphate, *J. Biol. Chem.* 283 (2008) 5677–5684.
- [39] B. Liu, D.F. Hassler, G.K. Smith, K. Weaver, Y.A. Hannun, Purification and characterization of a membrane bound neutral pH optimum magnesium-dependent and phosphatidylserine-stimulated sphingomyelinase from rat brain, *J. Biol. Chem.* 273 (1998) 34472–34479.
- [40] K. Hofmann, S. Tomiuk, G. Wolff, W. Stoffel, Cloning and characterization of the mammalian brain-specific, Mg²⁺-dependent neutral sphingomyelinase, *Proc. Natl. Acad. Sci. U. S. A.* 97 (2000) 5895–5900.
- [41] P. Deng, et al., Dietary inulin decreases circulating ceramides by suppressing neutral sphingomyelinase expression and activity in mice, *J. Lipid Res.* 61 (2020) 45–53.
- [42] Y.A. Hannun, L.M. Obeid, Sphingolipids and their metabolism in physiology and disease, *Nat. Rev. Mol. Cell Biol.* 19 (2018) 175–191.
- [43] S. Sindhu, et al., Neutral sphingomyelinase-2 and cardiometabolic diseases, *Obes. Rev. Off. J. Int. Assoc. Study Obes.* 22 (2021), e13248.
- [44] B.X. Wu, C.J. Clarke, Y.A. Hannun, Mammalian neutral sphingomyelinases: regulation and roles in cell signaling responses, *NeuroMolecular Med.* 12 (2010) 320–330.
- [45] A.A. Shamseddine, M.V. Airola, Y.A. Hannun, Roles and regulation of neutral sphingomyelinase-2 in cellular and pathological processes, *Adv. Biol. Regul.* 57 (2015) 24–41.
- [46] M.Y. Kim, C. Linaud, L. Obeid, Y. Hannun, Identification of sphingomyelin turnover as an effector mechanism for the action of tumor necrosis factor α and gamma-interferon. Specific role in cell differentiation, *J. Biol. Chem.* 266 (1991) 484–489.
- [47] D. Adam, K. Wiegmann, S. Adam-Klages, A. Ruff, M. Krönke, A novel cytoplasmic domain of the p53 tumor necrosis factor receptor initiates the neutral sphingomyelinase pathway, *J. Biol. Chem.* 271 (1996) 14617–14622.
- [48] A.E. Tcherkasowa, et al., Interaction with factor associated with neutral sphingomyelinase activation, a WD motif-containing protein, identifies receptor for activated C-kinase 1 as a novel component of the signaling pathways of the p53 TNF receptor, *J. Immunol.* 169 (2002) 5161–5170.
- [49] S.-Y. Lee, et al., Adipocyte-specific deficiency of de novo sphingolipid biosynthesis leads to lipodystrophy and insulin resistance, *Diabetes* 66 (2017) 2596–2609.
- [50] Y. Pewzner-Jung, et al., A critical role for ceramide synthase 2 in liver homeostasis: I. alterations in lipid metabolic pathways, *J. Biol. Chem.* 285 (2010) 10902–10910.
- [51] N. Marchesini, C. Luberto, Y.A. Hannun, Biochemical properties of mammalian neutral sphingomyelinase 2 and its role in sphingolipid metabolism, *J. Biol. Chem.* 278 (2003) 13775–13783.
- [52] G. Paolino, et al., Lipidic profile changes in exosomes and microvesicles derived from plasma of monoclonal antibody-treated psoriatic patients, *Front. Cell Dev. Biol.* 10 (2022), 923769.
- [53] S. Grösch, S. Schiffmann, G. Geisslinger, Chain length-specific properties of ceramides, *Prog. Lipid Res.* 51 (2012) 50–62.
- [54] Z. Dong, B.H. Lee, Bile salt hydrolases: structure and function, substrate preference, and inhibitor development, *Protein Sci. Publ. Protein Soc.* 27 (2018) 1742–1754.
- [55] A. Molinaro, A. Wahlström, H.-U. Marschall, Role of bile acids in metabolic control, *Trends Endocrinol. Metab.* 29 (2018) 31–41.
- [56] R.D. Berg, Bacterial translocation from the gastrointestinal tract, *Trends Microbiol.* 3 (1995) 149–154.
- [57] V. Lorenzo-Zúñiga, et al., Oral bile acids reduce bacterial overgrowth, bacterial translocation, and endotoxemia in cirrhotic rats, *Hepatology* 37 (2003) 551–557.
- [58] L.A. Woollett, et al., Cholic acid supplementation enhances cholesterol absorption in humans, *Gastroenterology* 126 (2004) 724–731.
- [59] J. Jiang, et al., Glycine- β -muricholic acid antagonizes the intestinal farnesoid X receptor-ceramide axis and ameliorates NASH in mice, *Hepatology* 6 (2022) 3363–3378.
- [60] K.R. Stayrook, et al., Regulation of carbohydrate metabolism by the farnesoid X receptor, *Endocrinology* 146 (2005) 984–991.
- [61] D. Duran-Sandoval, et al., The farnesoid X receptor modulates hepatic carbohydrate metabolism during the fasting-refeeding transition, *J. Biol. Chem.* 280 (2005) 29971–29979.
- [62] W.-S. Ge, et al., β -catenin is overexpressed in hepatic fibrosis and blockage of Wnt/ β -catenin signaling inhibits hepatic stellate cell activation, *Mol. Med. Rep.* 9 (2014) 2145–2151.
- [63] Y. Ishay, D. Nachman, T. Khoury, Y. Ilan, The role of the sphingolipid pathway in liver fibrosis: an emerging new potential target for novel therapies, *Am. J. Phys. Cell Phys.* 318 (2020) C1055–C1064.